# Large scale climate response Late Pliocene Ice Sheets as an Analogue for Future Climate: A Sensitivity Study of the Polar Southern Ocean and Antarctica to reduced ice sheetsHemisphere

Katherine Power<sup>1</sup>, Fernanda DI Alzira Oliveira Matos<sup>2</sup>, and Qiong Zhang<sup>1</sup>

**Correspondence:** Katherine Power (katherine.power@natgeo.su.se)

#### Abstract.

10

20

The Antarctic and Greenland Ice Sheets (AIS and GISGrIS) are critical tipping points in the Earth's climate system. Their potential collapse could trigger cascading effects, significantly alter the global climate patterns, and cause large-scale, long-lasting, and potentially irreversible changes within human timescales. This study investigates the large-scale climate response of the Southern polar Southern Hemisphere (pSH; comprising the Southern Ocean and Antarctica (60-90°S)) to the isolated effect of reducing ice sheet change in albedo resulting from reducing AIS and GrIS to prescribed Late Pliocene (LP) extent. Using well-documented paleogeography of the Late Pliocene (LP) LP from the PRISM4D reconstruction, where the West Antarctic Ice Sheet (WAIS) and the northwestern GIS GrIS were significantly diminished, we conducted 1450-year multicentennial simulations with the EC-Earth3 model at atmospheric CO<sub>T-2</sub> concentrations of 280 ppmv and 400 ppmv.

Our results reveal that the implementation of the LP ice sheet configuration extent leads to a 9.5°C rise in surface air temperature, approximately 16% reduction in sea ice concentration, and a 0.63 mm/day increase in precipitation over Antarctica and the Southern Ocean. These changes far exceed those driven by CO<sub>2-2</sub> increase alone, which result in a 2.5°C warming and a 9.3% sea ice decline. Throughout the simulations, the positive phase of the Under only CO<sub>2</sub>, there is a shift towards a more positive Southern Annular Mode (SAM)persists, intensifying westerly winds and contributing to sea ice export and deep ocean warming, supported by a strengthening of the westerly jet. However, CO<sub>2</sub> increase together with change in ice sheet extent results in a highly varied SAM, a result of a weakening and less stable westerly jet. The combined effects of ice sheet reduction and CO<sub>2</sub> forcing initially weakened 2 forcing initially reduce Antarctic Bottom Water formation, with major implications for the transport of water masses associated with the Global Meridional Overturning Circulation due to stronger water column stratification driven by surface freshening and subsurface warming.

By isolating the direct albedo effect of reducing GIS GrIS and AIS extents, this study offers critical insights into the mechanisms driving atmospheric and oceanic variability around Antarctica and their broader implications for global climate dynamics. Although the complete Late Pliocene boundary conditions may serve as a valuable analogue for current and future climate change, excluding the orographic changes allows us to specifically assess the primary role of surface reflectivity. This targeted approach lays the groundwork for future research to explore how the combined effects of albedo and paleogeographical changes could influence interhemispheric climate feedbacks under scenarios of future ice sheet collapse or instability.

<sup>&</sup>lt;sup>1</sup>Department of Physical Geography and Bolin Centre for Climate Research, Stockholm University, Stockholm, Sweden

<sup>&</sup>lt;sup>2</sup>Alfred Wegener Institute - Helmholtz Centre for Polar and Marine Research, Bremerhaven, 27570, Germany

#### 1 Introduction

35

Their high albedo reflects a significant portion of solar radiation, thereby cooling surrounding regions and playing a critical role in regulating global air and sea surface temperatures. In addition, these ice sheets influence atmospheric and oceanic processes by driving ocean circulation at various scales, modulating rates of sea ice and dense water formation, which are essential elements of global thermohaline circulation deep water formation as well as the wind regime across different oceanic basins (Clark et al., 1999). However, the stability of these ice sheets is increasingly at risk currently at risk due to enhanced melting of their ice, reduction in snowfall, and basal melting of ice cavities that happen due to climate change and are projecting to intensify in the following decades (Pollard et al., 2015; Song et al., 2025).

Projections indicate that the accelerated melt of the GIS and AIS, coupled with the retreat of their associated ice shelves (Naughten et al., 2023; Greene et al., 2024), loss of the GrIS and AIS will have far-reaching implications for global climate dynamics (Buizert et al., 2018) (Naughten et al., 2023; Greene et al., 2024; Buizert et al., 2018). These changes are likely to disrupt critical processes such as deep-water formation and the contribution of the southern ocean Southern Ocean to global heat and carbon transporttransport and carbon sequestration (Cai et al., 2013; Menviel et al., 2023). Understanding these risks is critical, as the potential collapse of the AIS and GIS GrIS could trigger cascading climate feedbacks, leading to irreversible and long-lasting changes within human timescales.

Paleoclimate records offer unique insights into the behavior of these ice sheets during past warm periods, such as Marine Isotope Stage 5e (~125,000 years ago) in the Pleistocene (Steig et al., 2015) and the Late Pliocene epoch Age (LP ~3,3 million years ago) (Naish et al., 2009; Kim and Crowley, 2000). These periods were characterised by significantly smaller ice sheets than today. Using these periods as analogs, we can better understand how ice sheet dynamics influence oceanic and atmospheric processes during these past warm periods in climates warmer than today, which can offer valuable lessons for predicting future climate behavior as the Earth continues to warm.

Paleoclimate insights from the Late Pliocene are increasingly used as analogues for future warm climate states, offering critical context for how Earth's climate system may respond to elevated CO<sub>2</sub> levels. Studies focusing on the Greenland Ice Sheet have demonstrated the importance of surface albedo feedbacks when considering future climate change, based on LP evidence (Power et al., 2023), de Nooijer et al. (2020) investigation of Arctic conditions during the LP gives insight to future conditions, as does Feng et al. (2017) work identifying amplified LP Arctic warming through key oceanic gateways, and Lunt et al. (2012) understanding of Pliocene polar amplification has aided our knowledge of amplification in a prospective warming world. Both Chandan and Peltier (2018) and Lord et al. (2017) demonstrate how bridging LP knowledge and future projections improve our understanding. In the Southern Hemisphere, the role of the Antarctic Ice Sheet in modulating future climate is gaining attention. Weiffenbach et al. (2024) show that mid-Pliocene simulations with a reduced AIS result in substantial Southern Ocean warming. This is primarily driven by sea ice loss, leading to stronger surface stratification and a weakening of the deep abyssal overturning circulation. Such changes in ocean structure and circulation provide valuable lessons for interpreting future AIS retreat under global warming. Building on these studies, our work offers a unique contribution by isolating the impact

of surface reflectivity changes associated solely with GrIS and AIS reduction, independently of topographic or vegetation feedbacks, and without freshwater inputs. This allows us to better understand how albedo feedbacks influence ocean-atmosphere interactions in the Southern Hemisphere in a warmer world.

In this study, we apply Late Pliocene ice sheet configurations to a modern geographic framework using sensitivity experiments with the EC-Earth model. replace the modern ice sheet mask of the EC-EARTH3 model with that of the Late Pliocene reconstruction provided by the Pliocene Model Intercomparison Project, phase 3 (PlioMIP3; (Haywood et al., 2024)). We do not modify, however, any other model boundary condition representative of the pre-industrial (PI; 1850 CE) Earth's geography. We perform sensitivity experiments applying these two ice sheet masks and multiple CO<sub>2</sub> concentrations. This approach allows us to assess the sensitivity of the climate system to changes in ice sheet extent and varying CO<sub>2-2</sub> concentrations, using ice sheet conditions of the past as an analogue for the future. By focusing on the albedo effect and excluding orographic changes, our goal is to uncover the key mechanisms and processes that could profoundly influence Earth's future climate, environment rand societies.

## 2 Model configuration and experiments setup

#### 2.1 Model configuration

80

85

We use the low-resolution configuration of the EC-Earth model, EC-Earth3-LR, an Earth System Model (ESM) developed collaboratively by the European research consortium EC-Earth. EC-Earth model has flexible configurations that allow for the inclusion or exclusion of various climate processes, making it a versatile tool for a wide range of climate studies (Döscher et al., 2022). EC-Earth3 integrates several key components, including the atmospheric model IFS cycle 36r4, the land surface module HTESSEL, the ocean model NEMO3.6 and the sea-ice module LIM3, all coupled via the OASIS3-MCT coupler. IFS and HTESSEL have a horizontal linear resolution of TL159 (1.125°), and the ocean and sea-ice components (NEMO and LIM) have a nominal resolution of 1° (Döscher et al., 2022).

The low-resolution configuration was selected to significantly reduce computational demandscosts, allowing for conducting multi-century-multi-centennial simulations and various sensitivity experiments. This setup is particularly suited for exploring slow processes in the deep ocean, which are central to the goals of this study. Such processes include changes in stratification, overturning circulation, and the response of Antarctic Bottom Water formation in response to altered climate forcing.

The EC-Earth3 model has consistently demonstrated its effectiveness in capturing key climate dynamics, including temperature variability, heat fluxes and other essential aspects of the Earth's System. This capability facilitates a more comprehensive understanding of the impacts of natural and anthropogenic forcing on the global climate system (Koenigk et al., 2013; Döscher et al., 2022; Cao et al., 2023). EC-Earth3 has been extensively validated in both modern and paleo-climate studies, showing robust performance in simulating the climates of past warm periods such as mid-Holocene, Last Interglacial and mid-Pliocene epochsLate Pliocene (Zhang et al., 2021; Chen et al., 2022; de Nooijer et al., 2020; Han et al., 2024). These simulations have provided valuable information that has been integrated to major model intercomparison projects, such as

PMIP4 (Paleoclimate Model Intercomparison Project phase 4) and PlioMIP2 (Pliocene Model Intercomparison Project phase 2) (Zhang et al., 2021; Chen et al., 2022; Power et al., 2023; Han et al., 2024) (Haywood et al., 2020, 2024).

## 2.2 Experiments setup

100

105

To investigate the impacts of varying ice sheet configurations extent and CO<sub>2</sub> concentrations in the Southern Ocean and Antarcticapolar Southern Hemisphere (pSH), we performed a series of sensitivity experiments, displayed in Table 1. These experiments employed modern ice-sheet configurations extent (labeled E) and Late Pliocene ice-sheet reconstructions ice-sheets (labeled Ei) under two atmospheric CO<sub>2</sub> levels: pre-industrial (280 ppmv) and intermediate (400 ppmv). Here we define the polar Southern Hemisphere as our domain of study. That includes the entire Southern Hemisphere from 60°S to 90°S.

The Late Pliocene Antarctic ice sheet reconstruction used in these experiments (Haywood et al., 2016; Chandan and Peltier, 2018)
were-

**Table 1.** The four Core and Tier 2 Pliocene for Future protocol experiments conducted. PI refers to pre-industrial conditions, LP for Late Pliocene. Name terminology is from (Haywood et al., 2016)

Experiment ID	Ice sheet extent	<u>LSM</u>	Topography	Vegetation	$CO_2$ (ppm)	Orbit
E280	₽Į	$\overset{\mathbf{PI}}{\sim}$	₽I	$ \underbrace{\mathbf{PI}}_{} $	280	$\overset{\mathbf{PI}}{\sim}$
<u>E400</u>	₽Į	$\overset{\mathbf{PI}}{\sim}$	₽I	$ \underbrace{\mathbf{PI}}_{} $	<u>400</u>	₽I
Ei280	LP.	₽Į	₽Ĭ	₽I	280	ΡĮ
Ei400	<u>LP</u>	₽Į	₽Ĭ	$\bigotimes$	<u>400</u>	₽Ĭ

The protocol for our pre-industrial (PI) simulation follows Eyring et al. (2016) framework for the Coupled Model Intercomparison Project version 6 (CMIP6) *piControl* experiment. Ice sheets, land geography, topography and vegetation are all unmodified from the model. GHG concentrations for CO<sub>2</sub>, CH<sub>4</sub> and N<sub>2</sub>O are 284.3 ppmv, 808.2 ppbv, and 273.0 ppbv, respectively. For orbital parameters; eccentricity set at 0.016764, obliquity 23.549 and perihelion - 180 is 100.33.

The aim of these sensitivity experiments is to unveil the isolated impact of abruptly shrinking of the AIS and GrIS to the climate of the polar Southern Hemisphere. Therefore, Ei simulations involve changing only ice sheet extent for the Greenland Ice and Antarctic Ice Sheets (Haywood et al., 2016; Chandan and Peltier, 2018). LP AIS was originally developed using the high-resolution British Antarctic Survey Ice Sheet Model, integrated with climatologies from the Hadley Centre Global Climate Model (Hill et al., 2007; Hill, 2009), utilising PRISM2 boundary conditions (Dowsett et al., 1999). The mid-Pliocene Greenland Ice Sheet (GIS) reconstruction Figure 1 provides a visual comparison of the modern and LP ice sheet extent LP GrIS reconstruction is provided for PlioMIP2 Haywood et al. (2016) is and based on 30 modelling results from the PLIS-MIP project Dolan et al. (2012). Given the focus of this study on the domain south of 60°S (Antarctic sector hereafter), Power and Zhang (2024) provides more detail, including spatial configuration of the effects of Greenland ice sheet are not explored in depth.

To isolate the impact of surface reflectivity (albedo), we excluded orographic changes and freshwater input associated with reduced ice sheet extent. This decision enables a targeted investigation of energy balance changes solely by surface albedo. Figure 1 provides a visual comparison of the modern and Pliocene ice sheet configurations. LP GrIS.

The PlioMIP ice sheet mask was interpolated onto the grid of EC-Earth's atmospheric component, IFS, and substituted into the snow depth variable of the initial condition file. IFS does not have a specific variable for ice sheets, therefore, altering the snow depth provides only a change in the ice sheet extent, being ice sheets the regions where snow depth exceeds 10 metres. To solely focus on climatic feedbacks resulting from change of AIS and GrIS; albedo values and ice sheet orography were not modified, and accompanying freshwater hosing experiments to account for meltwater from ice sheet change were not performed. With these exclusions, we aim to create idealised sensitivity experiments.

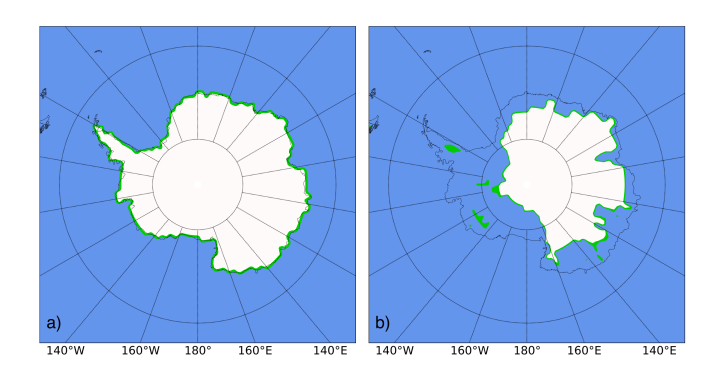


Figure 1. Comparison of the modern and Pliocene-LP Antarctic ice sheets sheet extent as provided by the PLISMIP project.

These simulations are part of the Pliocene for Future (P4F) Tier 2 experiments (Haywood et al., 2016), which has been proposed for the second phase of the Pliocene Model Intercomparison Project (PlioMIP2) and will be included in the new PlioMIP3 experiment list. The reliability of the Antarctic ice sheet configuration extent is further supported by the results of the PLISMIP results, which evaluated the dependencies of the ice sheet model for the warm period of the mid-Pliocene using 30 different models (Dolan et al., 2012). To ensure consistency across all simulations, modern vegetation, as simulated for the year 1850 CE, was fixed using the off-line LPJ-GUESS dynamic vegetation model (Chen et al., 2021). Each simulation spans a minimum of 1450 years, with the final 200 years of model output used for analysis of the mean state. The pre-industrial configuration (E280) serves as the PI control experiment for comparison.

3 Antarctica and The polar Southern Ocean Hemisphere response to increased CO<sub>2</sub> forcing 2 and LP ice sheet reductionsheets

#### 135 3.1 Near Surface Processes

120

Temperature, sea ice concentration and albedo anomalies resulting from increased CO<sub>2</sub> levels and the reduction of the modern ice sheet to Pliocene size. a) E400-E280 surface air temperature, b) Ei400-E280 surface air temperature, c) E400-E280 albedo,

d) Ei400-E280 albedo, e) E400-E280 sea ice concentration, f) Ei400-E280 sea ice concentration. White areas indicate results are not statistically significant at the 95% confidence level.

The interactions between the atmosphere, cryosphere and ocean are crucial in understanding how changes in CO<sub>2</sub> levels and ice sheet configurations influence climate feedbacks. Surface warming driven by both atmospheric and albedo changes directly impacts oceanic processes, particularly in the Southern Ocean. The delicate balance between surface stratification and deep water formation in this region is critical to regulating global ocean circulation, the influence of increased atmospheric CO<sub>2</sub> concentrations and reduced ice sheet extent on climate feedbacks in the polar Southern Hemisphere.

The simulations reveal that the near surface air temperature (TAS) increases by

## 3.1 Changes to temperature, albedo and sea ice concentration

145

150

155

160

165

170

In the E400 scenario (400 ppm CO<sub>2</sub>, relative to E280), average Antarctic surface air temperature rises by 2.51°C. The warming is most pronounced in two specific hotspots - Weddell and Ross seas, with temperatures increasing up to 6°C in the Weddell Sea (50°W, 75°S) and 5°C in the Ross Sea (160°W, 73°S) (figure 2a). Changes to albedo (Figure 2c) are primarily confined to these regions, with the most significant decrease (up to 20%) occurring in the Weddell Sea, extending between the coastline to 60°S, and clustered to the coastline moving eastward. A smaller area of albedo decline (10%) is observed west of the Ross Sea. Sea ice loss replicates these patterns surrounding the hotspots. Largest sea ice decline occurs to the east of the Weddell Sea (Figure 2e) and clustered to the coastline moving eastward, and a smaller area of sea ice loss found west of the Ross Sea. More moderate warming occurs across the majority of the remaining area, with generally less than 2°C increase over the interior of Antarctica and less than 1°C at the periphery of east Antarctica. This is accompanied by close to zero changes in albedo. A localised cooling of 1–2°C under increased CO<sub>2</sub> (E400 relative to E280; Figure 2a). However, when Pliocene ice sheet configurations are applied is observed in the southern ocean between 160°W-160°E, 62°S, where a small loss in albedo is also displayed (Figure 2c).

With LP ice sheet extent (Ei400 relative to E280), the warming intensifies, reading warming is much greater than E400; Antarctic near-surface air temperature increases by an average of 9.49°C(Figure 2b). Similarly, sea surface temperature (SST) increased by 1.26. The warming hotspots shift further inland, with temperatures rising by over 17°C under CO<sub>2</sub> forcing alone but increased to 4.89inland from the Ross Sea (180°–155°W, 81°–83°S) and up to 16°C with the combined effects of CO<sub>2</sub> and ice sheet changes (Figure ??a and b), compared to PI. These results underscore the amplified warming effect of reduced ice sheet extent compared to CO<sub>2</sub> increase alone, inland from the Weddell Sea (20°–35°W, 81°–83°S) (Figure ??b). The Ross and Weddell Seas themselves experience warming of up to 12°C and 13°C, respectively. The most substantial albedo declines occur at these inland hotspots; greater than 50% decline inland of the Ross Sea, whilst the Ross Sea itself experiences 30% decrease. There is an albedo reduction of 40-50% inland of the Weddell Sea, which extends into the Weddell Sea itself (Figure 2d). Sea ice losses are most drastic in these locations, with over 65% decline in the Weddel and 60% in the Ross Sea. High areas of sea ice loss are observed extending eastward from the Weddell Sea and westward from the Ross Sea.

Sea Surface Temperature (SST), sea level pressure (SLP) and precipitation anomalies resulting from increased CO<sub>2</sub> levels and the reduction of the modern ice sheet to Pliocene size, a) E400-E280 SST, b) Ei400-E280 SST, c) E400-E280 SLP, d)

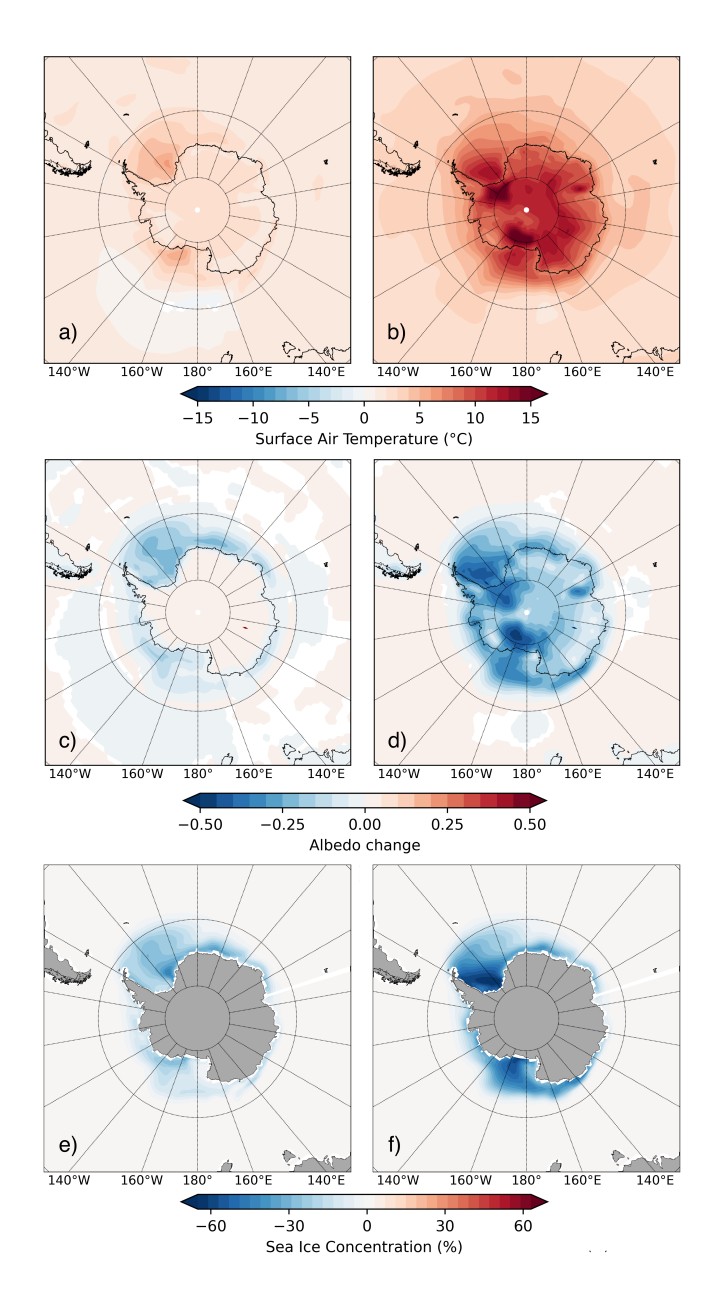


**Figure 2.** Temperature, Albedo and Sea Ice Concentration (SIC) variables from the only increased CO<sub>2</sub> level experiment and combined CO<sub>2</sub> and LP Ice Sheet extent, compared with the PI control. a) E400-E280 surface air temperature, b) Ei400-E280 surface air temperature, c) E400-E280 albedo, d) Ei400-E280 albedo, e) E400-E280 Siconc, f)Ei400-E280 Siconc. Only results statistically significant at the 95% confidence level are displayed.

Ei400-E280 SLP, e) E400-E280 precipitation, f) Ei400-E280 precipitation. White areas indicate results are not statistically significant at the 95% confidence level.

The spatial pattern of TAS and SST warming strongly align with albedo changes (Figures2a and b, and ??a and b). Under elevated CO<sub>2</sub> (E400), albedo reductions are only due to sea ice loss, primarily in the Ross and Weddell Seas, leading to a 9.25% decline in sea ice concentration (Figure 2e). In contrast, the configuration of the Pliocene ice sheet induces a widespread decline in albedo throughout the Antarctic , resulting in a more Over the interior of Antarctica, warming reaches 11–12°C, decreasing towards the eastern coastline where temperatures increase by 6–7°C. In Ei400, albedo changes are not confined to regions affected by ice sheet change and there is an overall albedo decline of 20% across the Antarctic interior, with decreasing severity toward the eastern coastline. There is a small hotspot showing pronounced loss of sea ice of 16. 25% (Figure 2 f). The loss of sea ice further reinforces the warming through a positive albedo feedback mechanism, exposing more of the ocean surface to direct solar heating. 30-40% on the east coast ( 60°–70°E, 75°S). Additionally, albedo decreases of up to 30% are observed along the coastline at 0°–10°E and 140°–160°E. These widespread albedo reductions are a result of the interplay of climate feedbacks, with changes in cloud cover, atmospheric temperature and moisture transport influencing the radiation balance and surface reflectivity.

Precipitation patterns also exhibit significant changes. Under increased CO<sub>2</sub>, precipitation increases by 0.42 mm/day relative to the PI control simulation, with the highest increases along Antarctic coasts (Figure ??e). When ice sheet reductions are included, precipitation increases further to 0.63 mm/day (Figure ??f), driven by enhanced atmospheric moisture transport. These changes are closely related to a persistent positive phase of the

## 3.2 Changes to regional atmospheric circulation patterns

180

185

190

195

200

205

As the surface temperature rises due to the abrupt change in radiative forcing applied through our experiments, the subsequent shifts in the climate create significant feedbacks that can influence large-scale atmospheric circulation, particularly the Southern Annular Mode (SAM)(Figure 4), which intensifies the westerly winds and enhances moisture convergence around the Antarctic.

The positive SAM phase also influences the . SAM is the leading mode of atmospheric variability in the Southern Hemisphere, characterised by fluctuations in the strength and position of the westerly winds encircling Antarctica. It has a large influence on pSH climate, sea ice cover and ocean circulation. Therefore, understanding how it responds to increased CO<sub>2</sub> concentrations and ice sheet changes is vital. Here we derive SAM mean state anomaly of the sensitivity experiments in relation to PI (Figure 3) by applying Empirical Orthogonal Functions (EOF) to the Sea Level Pressure (SLP) patterns. Elevated CO<sub>2</sub> levels lead to a mean reduction in SLP of 0.55 hPa over Antarctica and the surrounding Southern Ocean, reflecting the weakened high-pressure system due to atmospheric warming (Figure ??e). Conversely, reduced ice sheet extent results in a mean SLP increases of 1.37 hPa in most of Antarctica Figure ??d), strengthening the pressure gradient between the pole and mid-latitudes and intensifying westerly windsfield and extracting its first mode. SAM variability in the form of a timeseries spanning 200 years (Figure 4) was extracted through the first Principal Component of the EOF (PC1), standardized using a Savitzky-Golay filter.

In the control scenario, SAM (Figure 4a) displays a relatively well balanced variability, oscillating between positive and negative phases, but with marginally more occurrences of positive SAM phases during the period. This is recognised with the spatial pattern of EOF1, aligning with a more positive SAM.

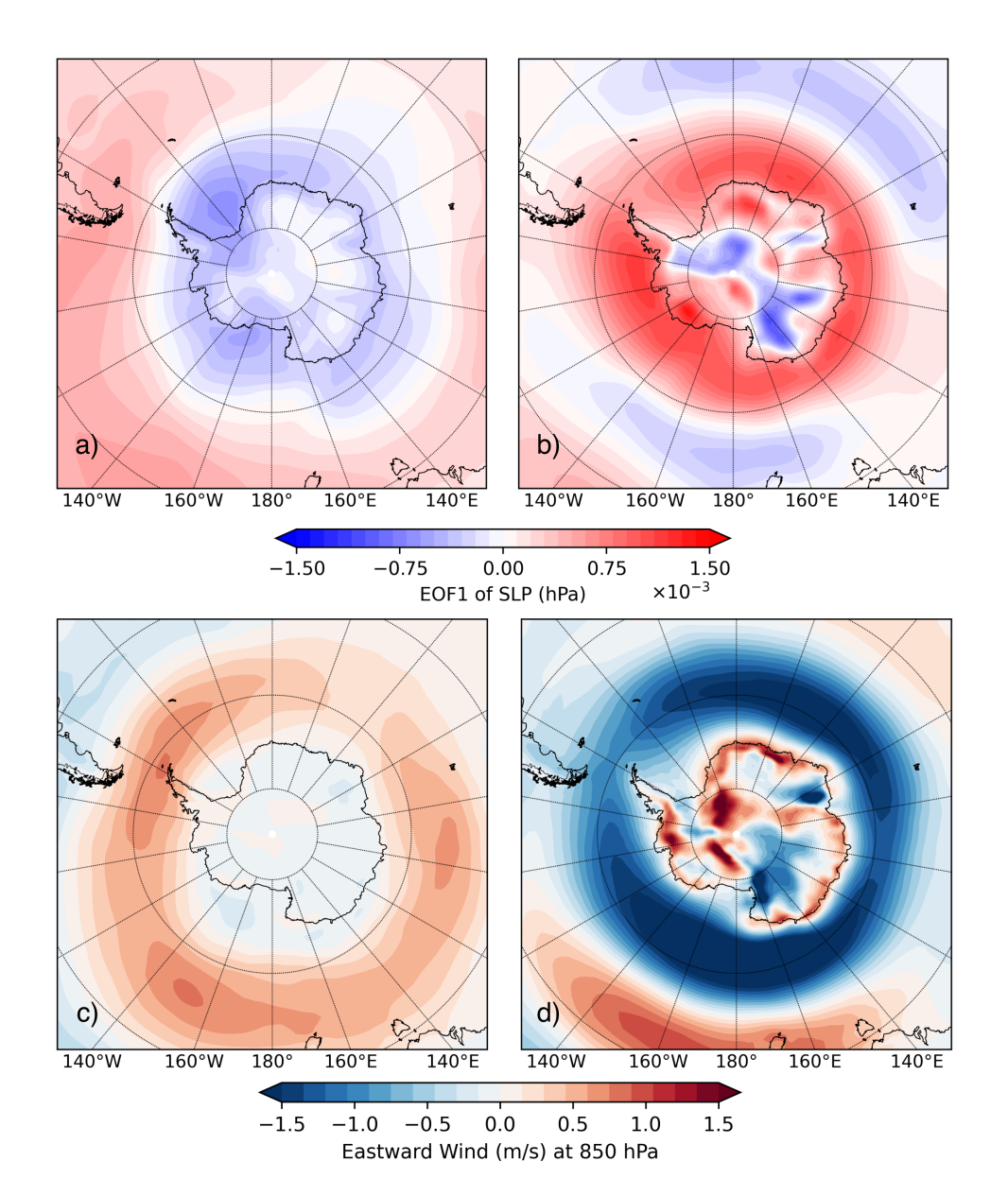


Figure 3. Anomaly (experiment - E280) of the (a,b) Southern Annular Mode mean state as the first EOF of the SLP in hPa; and (SAMc,d) index timeseries Eastward Wind speed at 850 hPa, for the E E400 and Ei Ei400 experiments. a) At 280 ppmv CO<sub>2</sub>. b) At 400 ppmv CO<sub>2</sub>. Thinner lines represent annual mean, while thicker lines are applied 10-year running to show the decadal variability respectively.

Under increased CO<sub>2</sub> (E400) there are more positive SAM events and fewer strong negative SAM phases, occurring over the time period compared to control, (Figure 4b). Spatially, a slightly stronger and more persistent SAM pattern is evident (Figure 3a), with an increase in pressure variability north of 60°S, consistent with stronger fluctuations in the westerly jet (Figure 3c),

the primary characteristic of a SAM positive phase. Pressure variability decreases south of 65°S, meaning a more stable polar vortex and reduced pressure fluctuations (Figure 3a).

A more positive SAM phase is typically associated with cooler temperatures over Antarctica in summer, as stronger westerly winds act as a barrier to warm air transport from lower latitudes. However, despite the shift toward a more positive SAM in E400, Antarctica still experiences warming (Figure 2a). This is likely due to the comparable forcing of the SAM index is small compared to the direct radiative forcing from increased CO<sub>2</sub>. Whilst the cooling effect of a positive SAM phase is strongest in summer, CO<sub>2</sub>-induced warming occurs throughout the year, leading to a net temperature increase despite the SAM shift. Plus, see ice declines may enhance warming that SAM cooling may not be able to compete with.

215

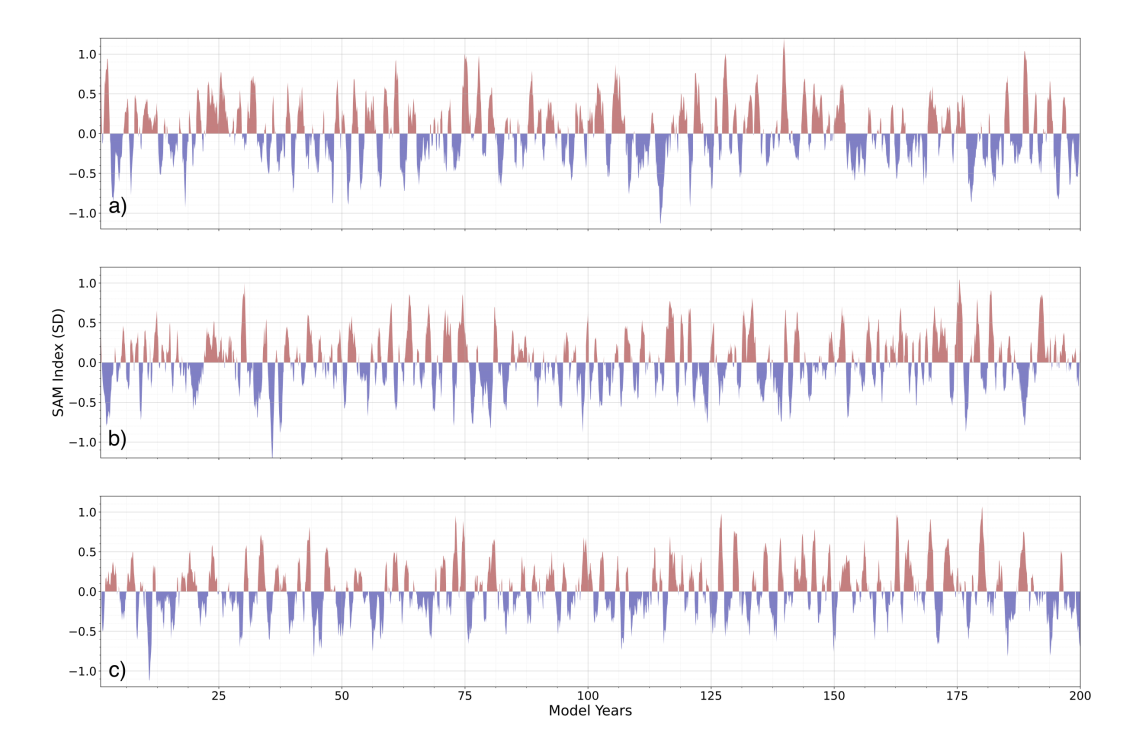


**Figure 4.** Timeseries of the Southern Annular Mode index derived from a Principal Component Analysis (PC1) for the a) E280, b) E400 and c) Ei400 experiments. The timeseries displays the last 200-year of the quasi-equilibrated simulations. The SAM index is filtered using a Savitzky-Golay filter.

This phase indicates acontraction of westerly winds towards Antarctica, causing an eastward shift and a deepening of the Amundsen sea low (Goddard et al., 2021), with stronger winds and stormier conditions in the Southern Ocean, the Antarctic Peninsula, the Bellingshausen Sea and the eastern Amundsen Sea (Fogt et al., 2011; Hosking et al., 2013; Raphael et al., 2016). Consequently, the influx of warm and moist maritime air into the west Antarctic increases precipitation while also contributing to regional warming and sea ice loss. The deepening of the Amundsen Sea Low enhances the northward export of sea ice in the Ross Sea. Simultaneously, the poleward contraction of westerlies drives increased upwelling of warm, deep ocean waters

in the Ross Gyre region. This upwelling accelerates sea ice melting from below, further amplifying surface warming due to sea ice loss, as seen in Figure 2. The loss of sea ice further lowers surface albedo, creating a positive feedback loop that accelerates warming. The exposed ocean surface absorbs more solar radiation, further intensifying the sea ice-albedo feedback and amplifying regional warming. Combining CO<sub>2</sub> with LP ice sheet extent, results in a greater variability of the SAM (Figure 4c), rather than a shift to a particular state. The distribution of events within the equilibrium period is broader, meaning both more extreme positive and negative SAM phases than control or E400. This indicates rather than a shift to one particular state, a more chaotic and less stable SAM pattern has emerged. EOF1 spatial pattern shows large increases in pressure variability from 60°S to the Antarctic coastline, (Figure 3b), supporting enhanced pressure fluctuations and a less stable atmospheric pattern. This change to the SAM stability is driven by a weakening of the SAM dominant control - the westerly jet (Figure 3d).

# 3.3 Southern Ocean-Sea Surface and deep water formation sensitivity to reduced AIS modified boundary conditions

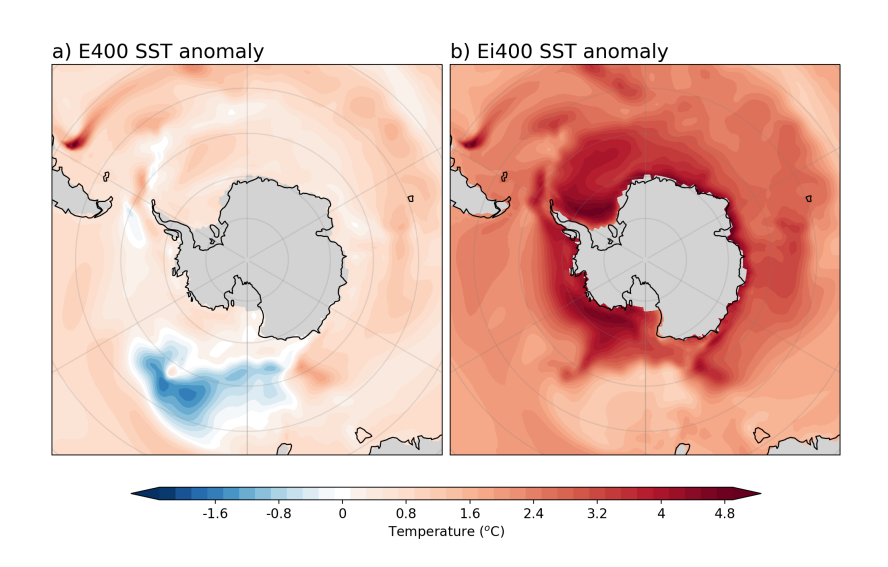


Figure 5. Time series Anomaly of the temperature and salinity of the Southern Ocean at Sea Surface Temperature (°C) in a) surface, E400 and b) 1km, c) 2km and d) 3km depths. Ei400 in relation to PI

#### Reducing the extent of the AIS

235

Changing the AIS and GrIS to LP extents has significant implications for Southern Ocean processes, particularly sea ice dynamics and deep-water formation. Although our model does not account for marine ice sheet instabilities, the loss of surface reflectivity and resulting albedo feedbacks are sufficient to induce notable changes in the Southern Ocean's stratification and overturning circulation.

processes occurring in the sea surface and deep waters of the polar Southern Hemisphere. At the surface —(0-10 meters), the ocean temperature does not reproduce the same warming in the hotspot regions as observed in Figure 2a. Rather than a more pronounced warming in the Weddel and Ross Seas, increasing the atmospheric CO<sub>2</sub> concentration to 400 ppmy results

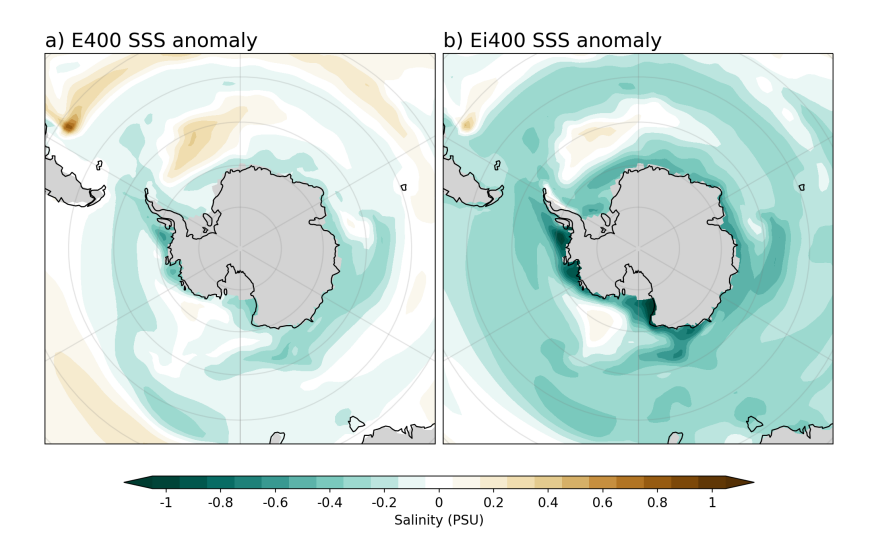


Figure 6. Anomaly of the Sea Surface Salinity (PSU) in a) E400 and b) Ei400 in relation to PI

in an overall warming along the path of the Antarctic Circumpolar Current (ACC), particularly within 45-55°S and through the Brazil-Malvinas Confluence (BMC) (Figure 5a). Under elevated CO<sub>2</sub> and LP ice sheet extent, sea surface warming (Figure 5b) agrees more consistently with air surface temperature change. The warm hotspot pattern seen at the Ross and Weddell Seas and Adelie coast is now evident, with SST increasing up to 5°C in the Weddell Sea. A warmer circle related to the reduction in sea ice is apparent. In the Ei400 experiment, the concentration of sea ice decreases by greater than 25% compared to PI (Figure 2 f), for some regions, exposing more of the ocean surface to direct solar heating. This warming contributes to apositive feedback loop, where the loss of sea ice lowers albedo, accelerates surface warming, and further reduces the extent of the sea ice. The sea surface temperature (SST) in Ei400 increases by up to 1°C relative to the start of the experiments. The salinity and temperature time series in figure 9 exhibit interannual to decadal variability, which may be linked to the interdecadal Pacific oscillation that dominates the variability of Southern Ocean SSTs on such a timescale (Yao et al., 2024)zonal heat transport promoted by the ACC around Antarctica within the latitudinal belt of 45-55°S is also evident.

Freshening of the Southern Ocean is another prominent feature of the reduced AIS experiment. The combination of enhanced precipitation and sea ice melt dilutes surface salinity, creating a stratified upper ocean layer that inhibits vertical mixing and deep water formation (Figure 9 In E400, the waters encircling Antarctica undergo an overall decrease in sea surface salinity (Figure 6a). This stratification has profound effects on deep convection processes, which are essential to ventilate the southern ocean and maintain the strength of Antarctic Bottom Water (AABW) formation. Surface salinisation occurs in the wind-driven outcrop of the Circumpolar Deep Water (CDW) associated with the Weddell gyre (located north of the Weddell Sea) and to a smaller extent the region associated with the Ross gyre. Salinisation of the upper ocean is also observed around the ACC path north of 55°S. Under Ei400 conditions, a decrease in salinisation is evident across the pSH (Figure 6b), with waters close to

the landmass undergoing the greatest decline in salinity. The only areas of salinisation are the wind-driven outcrop of the CDW associated with the Weddell and Ross Gyres, and the ACC path, although magnitudes are less than under E400.

Time series of the Antarctic Bottom Water formation index for experiments E400 and Ei400, calculated as the absolute value of the minimum global streamfunction south of 60°S and below 500 m depth (adapted from Zhang et al. (2019)).

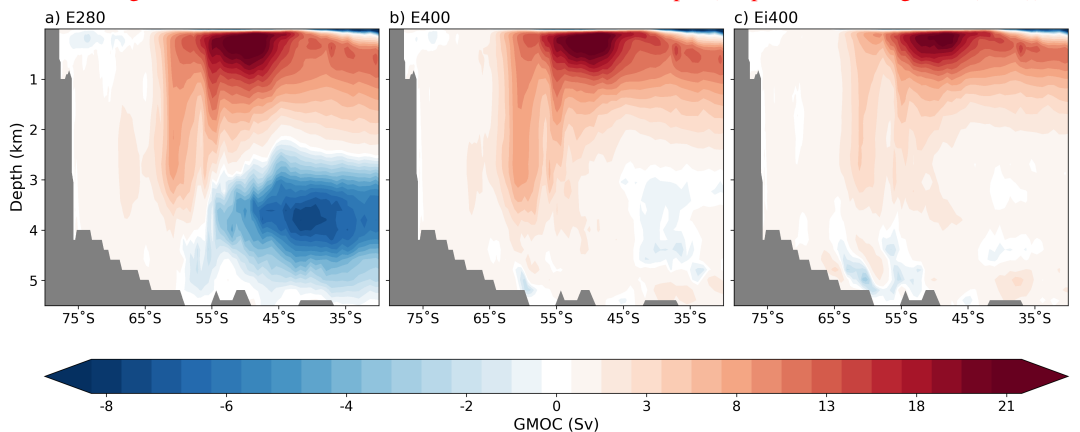


Figure 7. Southern Ocean MOC for the a) E280, b) E400, and c) Ei400 experiments averaged over the last 200 years of the simulation

265

270

275

280

Descending through the water column, temperature and salinity changes exhibit distinct patterns across depths. At 1 km, The CDW, represented by the clockwise circulation south of 55°S in Figure 7, is successively weakened under first elevated CO<sub>2</sub> and CO<sub>2</sub> forcing combined with changed ice sheet extent. The Southern Ocean Meridional Overturning Circulation (SMOC) also demonstrates a weakening of the AABW, from maximum combined strength in the subtropical ocean basins of 8 Sv. as opposed to barely reaching 2 km and 3 km depths, the seawater temperature increase by up to 1.5° relative to the beginning of the simulation (Figure 9. While surface layers show substantial freshening, deeper layers undergo initial salinisation for the first 700 years of the simulation, followed by a transition to freshening. This transition reflects the dynamic interaction between surface buoyancy fluxes, vertical mixing, and the redistribution of heat and salt within the Southern Ocean. Since neither the wind regime nor the Southern Ocean currents shifted significantly during our simulations, the thermohaline changes observed are primarily driven by the sea ice albedo feedback and the atmospheric greenhouse gas forcing. Sv in E400 and 4 Sv in Ei400. To further investigate AABW formation during runtime, we derive the time series of the AABW index (Figure ??). This index was calculated by deriving the absolute value of the minimum global streamfunction of the entire pSH domain, however below 500m depth (adapted from Zhang et al. (2019) to avoid incorporating surface overturning in our index.

The influence of the Antarctic continent on global ocean circulation is largely mediated through its intermediate and bottom water masses. Antarctic Intermediate Water (AAIW), and Antarctic Bottom Water (AABW). AABW, in particular, plays a critical role as it ventilates all major ocean basins Orsi et al. (1999). Understanding the processes governing its formation and variability is therefore essential for assessing the broader impacts of climate change.

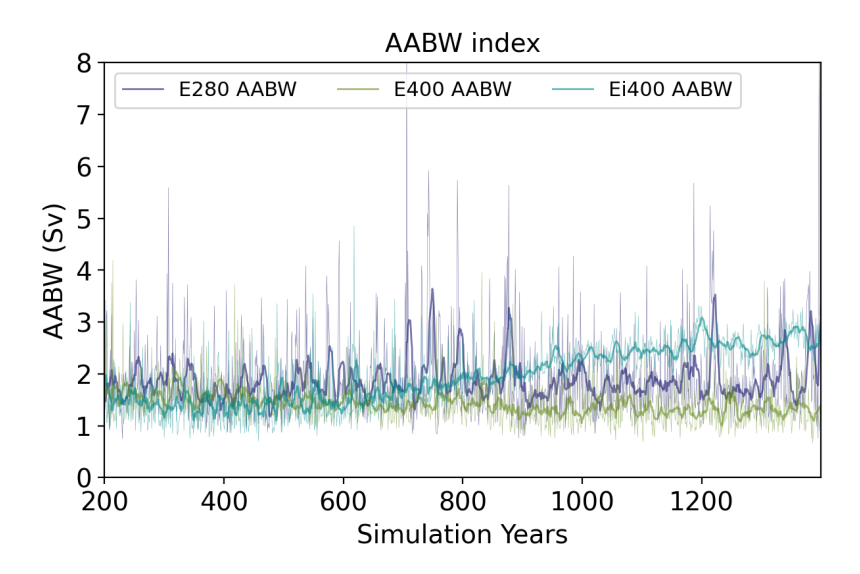


**Figure 8.** Time series of the Antarctic Bottom Water formation index for experiments E280, E400 and Ei400, calculated as the absolute value of the minimum global streamfunction of the pSH domain (60-90°S) and below 500 m depth (adapted from Zhang et al. (2019)).

A key consequence of these processes is the suppression of AABW formation. In both the Figure 8 reveals that the variability of AABW is strongly decreased in both E400 and Ei400 experiments, AABW strength, reduced by in relation to the E280 experiment and there is an initial AABW weakening of approximately 1 Sv  $(10^6 m^2 s^{-1})$  by year 700 of the simulationeompared to PI control (2 Sv) (figure 8). This reduction signifies a weakening of deep-water formation caused by increased stratification and reduced brine rejection during sea ice formation.

285

290

295

300

Interestingly, the AABW trends diverge in the later stages of the simulation. In the E400experiment, AABW continues to weaken, whereas in Ei400experiment, it begins to recover after year 700. This recovery suggests that the reduced AIS triggers LP ice sheets trigger a compensatory mechanism, likely involving the import of salinity into salinisation of the Southern Ocean at deeper levels, which enhances AABW strength on multi-centennial timescales, counteracting and counteracts the initial suppression. Figure 9g, confirms this hypothesis, as the Southern Ocean experiences increase in salinity during runtime at 3 km in the Ei400 experiment.

The broader impact for Global Meridional Overturning Circulation (GMOC) is evident in figure 7. The AABW cell, represented by the blue anticlockwise circulation at the bottom of the ocean, shrinks significantly in E400 but retains greater strength and coverage in the Analysing the temperature and salinity through the surface, intermediate, and deeper levels of the water column over time, there is an increase of ocean temperature of 1.5°C occurring at 1, 2 and 3 km depths, relative to the beginning of the simulation (Figures 9b, d, f and h). The degree of warming is about 2°C higher in Ei400 experiment (figures 7band 7c). This pattern aligns with the findings of (Sidorenko et al., 2021), where surface buoyancy loss, ozone depletion, and stronger westerlies over the Southern Ocean inhibit AABW formation and export. However, our simulations suggest that the reduced AIS not only amplifies surface-driven feedbacks but also initiates deep-ocean processes that partially mitigate the

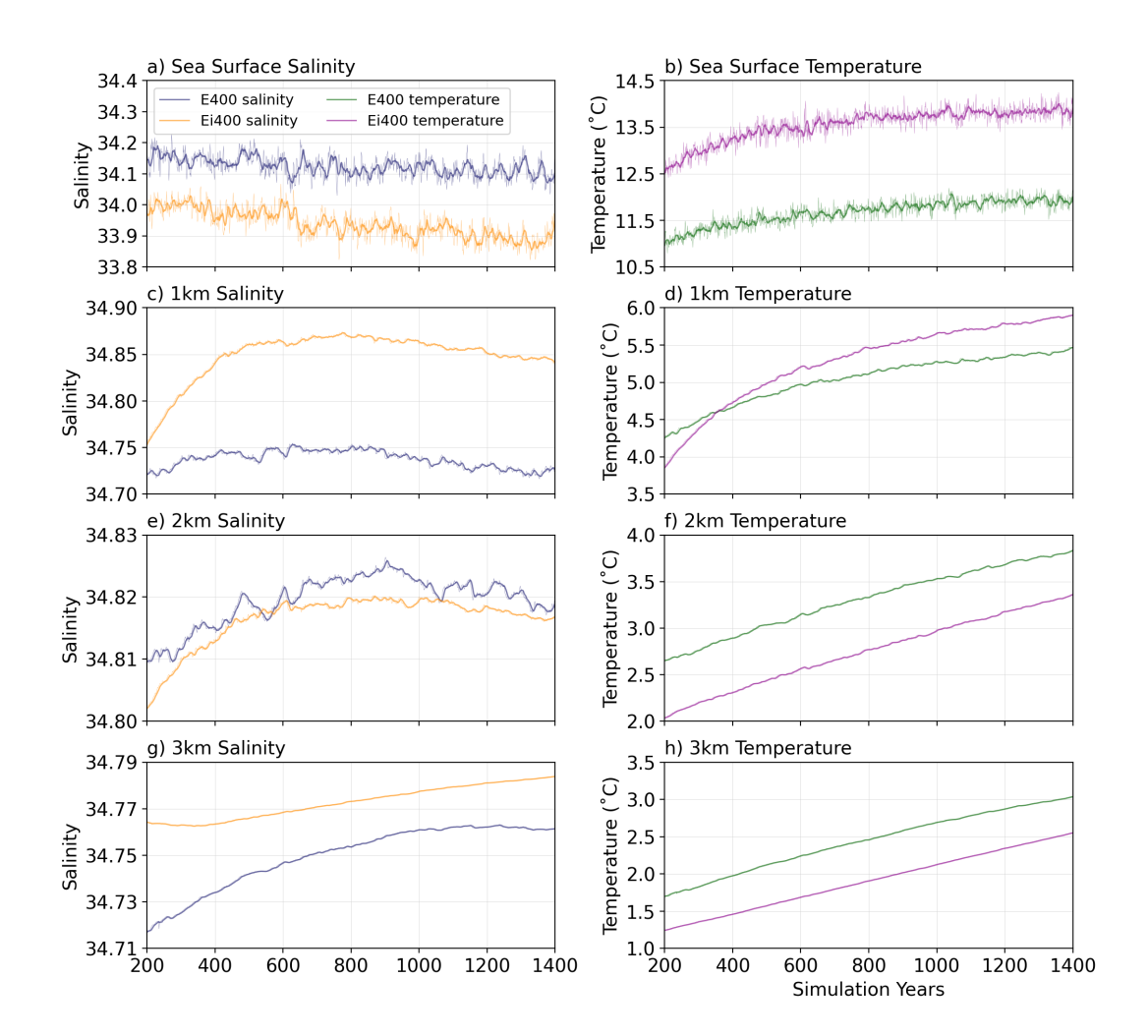


Figure 9. Southern Ocean MOC for Time series of the asalinity and temperature of the of the pSH domain (60-90°S) E280at (a,b) E400surface, and (c,d) Ei400 experiments during averaged over the last 200 years of the simulation lkm, (e,f) 2km and (g,h) 3km depths.

suppression of deep-water formation than in E400. The surface layers show substantial freshening, whilst deeper layers undergo initial salinisation for the first 700 years of the simulation (Figures 9 a, c, e and g), followed by a transition to freshening, except for 3 km.

In particular, our simulations do not indicate significant changes in the wind regime over Antarctica or the Southern Ocean.

This absence suggests that the observed effects are mainly driven by changes in surface buoyancy due to the combined impact of  $CO^2$  forcing and ice sheet loss. In contrast to scenarios where strengthened winds amplify surfacebuoyancy loss, our model reproduces a similar state through thermohaline feedbacks alone. Furthermore, removing such a large extent of the AIS induces an amplified buoyancy gain response in the deep ocean, which counterbalances the strengthening of the upper overturning cell

over multi-centennial timescales. This response highlights the role of salinity import in enhancing the strength of AABW under the condition of reduced ice sheet extent.

#### 4 Discussion

310

320

325

330

335

340

In E400 Antarctic warming is modest overall. Air temperature changes are most pronounced in areas with sea ice loss and therefore albedo declines, such as the Weddell Sea. This surface warming flattens the local temperature gradient (Kidston et al., 2011), meaning a weaker local baroclinicity and a reduction in eddy generation and therefore lower pressure variability (Figure 3a). The loss of sea ice contributes to a smoother surface, further weakening baroclinicity and suppressing storm development (Screen et al., 2011). Pressure increases around 50–60°S, and the westerly jet strengthens, showing a shift to a more positive SAM phase. This pattern is consistent with observational and modeling studies, which show a positive SAM in response to greenhouse forcing (Thompson et al., 2005; Marshall, 2003)).

intense interior mixing (Tamsitt et al., 2017), encouraging upwelling of colder, yet fresh, deeper water from the abyssal Pacific (aided by topographic constraints imposed by the Macquarie and Pacific-Antarctic Ridges). This contributes to the Pacific cooling evident on both Figure 2 and 5. The sea ice loss here drives a contraction of the seasonal Sea Ice Zone (SIZ) and reduces Antarctic Divergence (Ramadhan et al., 2022), ultimately meaning a decline in upwelling of warm CDW further leading to the cooling Pacific hotspot. This behaviour is consistent with current observations (Beadling et al., 2022; Roach et al., 2023; Schmidt et al., 2023; By increasing stratification at deep convection sites, and inhibiting the vertical mixing required for deep-water formation. This self-reinforced mechanism amplifies—, the positive phase of the SAM is amplified, intensifying the effects of atmospheric circulation that contribute to regional warming and increased precipitation—around Antarctica at elevated  $CO_2$  levels. However, these processes are insufficient to fully balance the salinisation that occurs in the deep ocean, which remains a key challenge for the recovery of deep-water formation.  $CO_2$  levels.

In general, ocean warming driven by a negative sea-ice albedo feedback increases. The stronger westerlies promote more

Although our simulations represent idealised scenarios, the results underscore the critical sensitivity. In Ei400 an intense southern polar warming leads to complex and regionally varying atmospheric responses. The strongest warming (up to 16°C) is located over and inland from the Ross and Weddell Seas, also showing largest albedo declines (up to 50%) and significant sea ice losses. Ocean temperatures show widespread warming; the topographic upwelling enforced by increased Ekman pumping observed in E400 is reduced not only from the decreased Antarctic Divergence but also from reduced overall vertical mixing. Stratification is enhanced due to substantially warmer and fresher surface waters (Figure 6b). The mild freshening of Weddell and Ross Gyres connects to the weakening of CDW, as both gyres contribute to poleward heat transport and therefore increased sea ice melt, a decreased upwelling and poleward transport of warmer waters.

It is this freshening and warming of the upper ocean, coupled with sea ice loss, which weakens the AABW. The AABW formation is a process that depends largely on sea-ice dynamics and the interplay between salinity and temperature in the water column. Under stable conditions, the freshwater fluxes induced by sea-ice melting during summer are balanced by the cold temperatures of the Southern Oceanto increased atmospheric warming. Current conditions do not yet reflect the full extent of

AIS reduction or collapse, as projected in future climate experiments Roach et al. (2023); Armstrong McKay et al. (2022); Naughten et al. . However, our results suggest that even under present trends, the ability of , whereas the salinity increase induced by brine rejection during sea-ice formation in winter densifies the water column. Such cold dense water mass then moves towards the ocean bottom layer (Silvano et al., 2023). Ocean stratification and reduced brine rejection that happens during sea ice formation and therefore limits AABW formation (Talley, 1993). These results align with the findings of (Sidorenko et al., 2021), where surface buoyancy loss and stronger westerlies over the Southern Ocean inhibit AABW formation and export. These findings suggest that the Southern Ocean to ventilate the deep ocean is at significant risk. Furthermore, while we isolate the albedo effect in this study to reduce uncertainties, the exclusion of other climate feedbacks may underestimate the potential catastrophic outcomes of AIS collapse. These insights are vital for tuning climate models and reconciling data-model discrepancies reduced ice sheets not only amplify surface-driven feedbacks but also initiate deep-ocean processes that partially mitigate the suppression of deep-water formation The Ei400 AABW recovery suggests that LP ice sheets trigger a compensatory mechanism involving the salinisation of the Southern Ocean at deeper levels, to enhance AABW strength and counteract the initial suppression.

Regions exhibit different behaviors of SLP variability. Inland from the Weddell Sea, we observe a decrease in SLP variability. This suggests a breakdown of the local temperature gradient, weakening baroclinicity and reducing the strength of transient eddies consistent with E400 and Kidston et al. (2011). Inland from the Ross sea however, pressure variability increases, indicating other regional dynamics such as katabatic winds. Notably, we observe adjacent zones of both wind strengthening and weakening, pointing to disrupted and complex wind regimes around Antarctica, particularly over the continent itself. These non-zonally symmetric changes in both winds and pressure patterns, are consistent with the idea that regional feedbacks and non-linearities emerge once the ice sheet is reduced.

## 5 Late Pliocene ice sheets as analogues for future climate

The GIS and AIS are undergoing dramatic changes due to polar amplification (Armstrong McKay et al., 2022). If the current pace of radiative forcing continues, the potential collapse of these ice sheet could trigger complex climate feedbacks. These include increased meltwater input, surface cooling, changes in westerly wind patterns, and multi-centennial variability in sea-ice production. Although some feedbacks may eventually promote the recovery of deep-water production when a certain threshold is reached (Johnson et al., 2024; Aylmer et al., 2022; Kang et al., 2023), the pathways to such recovery remain highly uncertain. Further north, in the circumpolar Southern Ocean between 50°–60°S, there is a weakening of the westerly winds. This aligns with the reduction in the equator-to-pole temperature gradient, which weakens the zonal pressure gradient that drives the westerly jet. In Ei400, the tropical regions warm by 2.32°C, but Antarctica warms by 9.18°C, drastically reducing the meridional temperature contrast from 42.1°C in the control to 37.3°C. A weakening of the gradient leads to a weaker, more meandering jet and a less stable SAM pattern (Thompson and Wallace, 2000; Gerber and Vallis, 2007). This explains the observed weakening of the zonal winds and the increase in SAM variability—a signature of a less coherent, more fluctuating SAM state. This weakening of the westerlies also substantially impacts the advection of surface warmer waters by the ACC.

and leads to a decrease in formation of coastal polynyas that contribute to sea ice formation and salinisation of the deeper layers of the Southern Ocean (Kusahara et al., 2017).

## 5 Late Pliocene ice sheets as analogues for future climate

375

380

385

390

395

400

405

There is a notable gap in existing research on the isolated impact of the abrupt removal of large portions of AIS and GIS GrIS on climate and ocean circulation. The Late Pliocene epoch Age serves as an important analogue of future climate scenarios due to its modern-like atmospheric CO<sub>2-2</sub> concentrations, significantly reduced ice sheets , comparable ocean gateway configurations, and ecosystem shifts. This paleogeographic framework offers a valuable opportunity to assess climate sensitivity to regional albedo changes. In this study, we specifically isolate the albedo effect of ice sheet reduction to examine its role in driving Antarctic climate dynamics and Southern Ocean circulation. A PlioMIP-conform idealised sensitivity experiment would incorporate the orography changes that would accompany the reduction in ice sheet. Under future ice sheet loss, the changes in orography that will result are likely to have significant impacts on the surrounding climate and Southern Ocean. Here, we choose to not include orographical change however. The additional uncertainties from both deriving the parameters needed to modify orography in the model (including adjusting mean orography in the atmospheric component and sub-grid scale parameters such as standard deviation, slope, and angle) and from whether future orographical changes will closely align with those reconstructed for the Late Pliocene, may outweigh the benefits of an idealised sensitivity experiment. Our simulations with isolated PRISM4D ice sheet conditions demonstrate that ice sheets play a critical role in modulating climate feedbacks in response to warming.

The configuration of the Pliocene ice sheet results in a substantial Antarctic warming of 9.5°C, an increase in SST by 4.9°C, a loss of 16, 2% sea ice, and a rise in precipitation by 0.63 mm/day. As expected, the atmospheric and oceanic responses observed in our sensitivity experiments do not fully reproduce the climate changes seen in more comprehensive modeling studies that incorporate all boundary conditions of the Late Pliocene. Nor do they fully match the reconstructed climate based on proxy data (Burls et al., 2017; Haywood et al., 2013, 2016, 2024). However, current and future climates are not exact replicas of the Late Pliocene either. Thus, our conclusions focus on the idealised interactions of climate feedbacks in these controlled experiments. Therefore, point to point comparison needs to be done with caution. Our results do agree with the consensus from Pliocene Model Intercomparison Project (PlioMIP2), that the influence of a strongly reduced AIS exacerbates the changes induced by a higher CO<sub>2</sub> concentration alone. However, Weiffenbach et al. (2024) reported a Southern Ocean SST warming of 2.8°C according to PlioMIP2 ensemble, driven by reduced sea ice cover linked to AIS retreat. This value is less than our average of 4.89°C and agrees better with SST change from AIS melt and elevation change in the Last Interglacial (LIG) of 2°C Hutchinson et al. (2024). The mechanisms we establish, however, are paralleled in both paleo and current work. Our findings of a weakened SMOC, driven by surface layer freshening, and initial salinification at depth, agrees with findings by Yeung et al. (2024), of a weakened deep convection and subsurface warming during the LIG. A reduction in AABW is also established by Gorte et al. (2023). Whilst this experiment models freshwater discharge, the mechanism of enhanced stratification due to freshening suppressing deep convection aligns with our findings here.

Our decision not to include the orographical change associated with reduced ice sheets is based on two considerations: (1)

There is no clear indication that future orographical changes will closely align with those reconstructed for the Late Pliocene, even though strong evidence suggests ice sheet extent may be similar; (2) Modifying orography in models is a complex task that involves adjusting not only to mean orography in the atmospheric component but also sub-grid scale parameters, such as standard deviation, slopes, and angles. Deriving these parameters introduces additional uncertaintiesthat could outweigh the benefits of including orographic changes in an idealised sensitivity experiment.

## **6 Conclusions**

This study underscores the critical sensitivity of the Southern Ocean to increased atmospheric warming. Current conditions do

not yet reflect the full extent of AIS reduction or collapse, as projected in future climate experiments (Roach et al., 2023; Armstrong McKay

. However, our results suggest that even under present trends, the ability of the Southern Ocean to ventilate the deep ocean is

at significant risk. Furthermore, while we isolate the albedo effect in this study to reduce uncertainties, the exclusion of other

climate feedbacks may underestimate the potential catastrophic outcomes of AIS collapse.

This raises potential research questions for future investigation. We believe that an extended set of sensitivity experiments would provide valuable insights into future climate change and even reduce model biases. Experiments would include:

- 1. Freshwater hosing equivalent to the ice sheet volume that is reduced in LP relative to PI;
- 2. Application of reconstructed LP paleogeography (topography and bathymetry);
- 3. Increased greenhouse gas forcing;
- 4. Interactive ice sheets.
- Thus, we conclude that the reduction of AIS primarily influences the circulation of the Antarctic and Southern basins. By isolating the albedo effect, our study provides a foundational understanding of how ice sheet loss, independent of freshwater input and orographic changes, can significantly alter Southern Hemisphere climate dynamics. These insights are critical for refining future climate models and identifying early signals of ice sheet retreat, offering a clearer picture of the potential pathways and risks associated with polar ice sheet instability.
- Author contributions. Conceptualization, K.P., F.D.A.O.M., Q.Z.; methodology, K.P., F.D.A.O.M.; formal analysis, K.P., F.D.A.O.M.; investigation, K.P., F.D.A.O.M.; resources, K.P., Q.Z.; data curation, K.P.; writing–original draft preparation, K.P.; writing–review and editing, K.P., F.D.A.O.M., Q.Z.; visualization, K.P. F.D.A.O.M.; project administration, Q.Z.

Competing interests. The authors declare no conflict of interest.

Acknowledgements. This work was supported by the Swedish Research Council (Vetenskapsrådet, grant no. 2022-03129)

The data analyses were performed using resources provided by the ECMWF's computing and archive facilities and Swedish National Infrastructure for Computing (SNIC) at the National Supercomputer Centre (NSC), which is partially funded by the Swedish Research Council through grant agreement no. 2022-06725.

#### References

- Armstrong McKay, D. I., Staal, A., Abrams, J. F., Winkelmann, R., Sakschewski, B., Loriani, S., Fetzer, I., Cornell, S. E., Rock-ström, J., and Lenton, T. M.: Exceeding 1.5°C global warming could trigger multiple climate tipping points, Science, 377, eabn7950, https://doi.org/10.1126/science.abn7950, 2022.
  - Aylmer, J., Ferreira, D., and Feltham, D.: Different mechanisms of Arctic and Antarctic sea ice response to ocean heat transport, Climate Dynamics, 59, 315–329, https://doi.org/10.1007/s00382-021-06131-x, 2022.
- Beadling, R. L., Krasting, J. P., Griffies, S. M., Hurlin, W. J., Bronselaer, B., Russell, J. L., MacGilchrist, G. A., Tesdal, J., and Winton,
   M.: Importance of the Antarctic Slope Current in the Southern Ocean Response to Ice Sheet Melt and Wind Stress Change, Journal of Geophysical Research: Oceans, 127, e2021JC017 608, https://doi.org/10.1029/2021JC017608, 2022.
  - Buizert, C., Sigl, M., Severi, M., Markle, B. R., Wettstein, J. J., McConnell, J. R., Pedro, J. B., Sodemann, H., Goto-Azuma, K., Kawamura, K., Fujita, S., Motoyama, H., Hirabayashi, M., Uemura, R., Stenni, B., Parrenin, F., He, F., Fudge, T. J., and Steig, E. J.: Abrupt ice-age shifts in southern westerly winds and Antarctic climate forced from the north, Nature, 563, 681–685, https://doi.org/10.1038/s41586-018-0727-5, 2018.
  - Burls, N. J., Fedorov, A. V., Sigman, D. M., Jaccard, S. L., Tiedemann, R., and Haug, G. H.: Active Pacific meridional overturning circulation (PMOC) during the warm Pliocene, Science Advances, 3, e1700 156, https://doi.org/10.1126/sciadv.1700156, 2017.
  - Cai, W., Zheng, X.-T., Weller, E., Collins, M., Cowan, T., Lengaigne, M., Yu, W., and Yamagata, T.: Projected response of the Indian Ocean Dipole to greenhouse warming, Nature Geoscience, 6, 999–1007, https://doi.org/10.1038/ngeo2009, 2013.
- Cao, N., Zhang, Q., Power, K. E., Schenk, F., Wyser, K., and Yang, H.: The role of internal feedbacks in sustaining multi-centennial variability of the Atlantic Meridional Overturning Circulation revealed by EC-Earth3-LR simulations, Earth and Planetary Science Letters, 621, 118 372, https://doi.org/10.1016/j.epsl.2023.118372, 2023.
  - Chandan, D. and Peltier, W. R.: On the mechanisms of warming the mid-Pliocene and the inference of a hierarchy of climate sensitivities with relevance to the understanding of climate futures, Climate of the Past, 14, 825–856, https://doi.org/10.5194/cp-14-825-2018, 2018.
- Chen, J., Zhang, Q., Huang, W., Lu, Z., Zhang, Z., and Chen, F.: Northwestward shift of the northern boundary of the East Asian summer monsoon during the mid-Holocene caused by orbital forcing and vegetation feedbacks, Quaternary Science Reviews, 268, 107 136, https://doi.org/10.1016/j.quascirev.2021.107136, 2021.
  - Chen, J., Zhang, Q., Kjellström, E., Lu, Z., and Chen, F.: The Contribution of Vegetation Climate Feedback and Resultant Sea Ice Loss to Amplified Arctic Warming During the MidHolocene, Geophysical Research Letters, 49, https://doi.org/10.1029/2022GL098816, 2022.
- 465 Clark, P. U., Alley, R. B., and Pollard, D.: Northern Hemisphere Ice-Sheet Influences on Global Climate Change, Science, 286, 1104–1111, https://doi.org/10.1126/science.286.5442.1104, 1999.
  - de Nooijer, W., Zhang, Q., Li, Q., Zhang, Q., Li, X., Zhang, Z., Guo, C., Nisancioglu, K. H., Haywood, A. M., Tindall, J. C., Hunter, S. J., Dowsett, H. J., Stepanek, C., Lohmann, G., Otto-Bliesner, B. L., Feng, R., Sohl, L. E., Chandler, M. A., Tan, N., Contoux, C., Ramstein, G., Baatsen, M. L. J., von der Heydt, A. S., Chandan, D., Peltier, W. R., Abe-Ouchi, A., Chan, W.-L., Kamae, Y., and Brierley, C. M.:
- Evaluation of Arctic warming in mid-Pliocene climate simulations, Climate of the Past, 16, 2325–2341, https://doi.org/10.5194/cp-16-2325-2020, 2020.
  - Dolan, A. M., Koenig, S., Hill, D. J., Haywood, A. M., and DeConto, R.: Pliocene Ice Sheet Modelling Intercomparison Project (PLISMIP) experimental design, Geoscientific Model Development, 5, 963–974, https://doi.org/10.5194/gmd-5-963-2012, 2012.

- Dowsett, H., Barron, J., Poore, R., Thompson, R., Cronin, T., Ishman, S., and Willard, D.: Middle Pliocene paleoenvironmental reconstruction: PRISM2, Tech. rep., USGS, http://pubs.usgs.gov/openfile/of99-535, 1999.
  - Döscher, R., Acosta, M., Alessandri, A., Anthoni, P., Arsouze, T., Bergman, T., Bernardello, R., Boussetta, S., Caron, L.-P., Carver, G., Castrillo, M., Catalano, F., Cvijanovic, I., Davini, P., Dekker, E., Doblas-Reyes, F. J., Docquier, D., Echevarria, P., Fladrich, U., Fuentes-Franco, R., Gröger, M., v. Hardenberg, J., Hieronymus, J., Karami, M. P., Keskinen, J.-P., Koenigk, T., Makkonen, R., Massonnet, F., Ménégoz, M., Miller, P. A., Moreno-Chamarro, E., Nieradzik, L., van Noije, T., Nolan, P., O'Donnell, D., Ollinaho, P., van den Oord,
- G., Ortega, P., Prims, O. T., Ramos, A., Reerink, T., Rousset, C., Ruprich-Robert, Y., Le Sager, P., Schmith, T., Schrödner, R., Serva, F., Sicardi, V., Sloth Madsen, M., Smith, B., Tian, T., Tourigny, E., Uotila, P., Vancoppenolle, M., Wang, S., Wårlind, D., Willén, U., Wyser, K., Yang, S., Yepes-Arbós, X., and Zhang, Q.: The EC-Earth3 Earth system model for the Coupled Model Intercomparison Project 6, Geoscientific Model Development, 15, 2973–3020, https://doi.org/10.5194/gmd-15-2973-2022, 2022.
- Eyring, V., Bony, S., Meehl, G. A., Senior, C. A., Stevens, B., Stouffer, R. J., and Taylor, K. E.: Overview of the Coupled Model

  Intercomparison Project Phase 6 (CMIP6) experimental design and organization, Geoscientific Model Development, 9, 1937–1958,

  https://doi.org/10.5194/gmd-9-1937-2016, 2016.
  - Feng, R., Otto-Bliesner, B. L., Fletcher, T. L., Tabor, C. R., Ballantyne, A. P., and Brady, E. C.: Amplified Late Pliocene terrestrial warmth in northern high latitudes from greater radiative forcing and closed Arctic Ocean gateways, Earth and Planetary Science Letters, 466, 129–138, https://doi.org/10.1016/j.epsl.2017.03.006, 2017.
- 490 Fogt, R. L., Bromwich, D. H., and Hines, K. M.: Understanding the SAM influence on the South Pacific ENSO teleconnection, Climate Dynamics, 36, 1555–1576, https://doi.org/10.1007/s00382-010-0905-0, 2011.
  - Gerber, E. P. and Vallis, G. K.: Eddy–Zonal Flow Interactions and the Persistence of the Zonal Index, Journal of the Atmospheric Sciences, 64, 3296–3311, https://doi.org/10.1175/JAS4006.1, 2007.
- Goddard, P. B., Tabor, C. R., and Jones, T. R.: Utilizing Ice Core and Climate Model Data to Understand Seasonal West Antarctic Variability,

  Journal of Climate, 34, 10 007–10 026, https://doi.org/10.1175/JCLI-D-20-0822.1, 2021.
  - Gorte, T., Lovenduski, N. S., Nissen, C., and Lenaerts, J. T. M.: Antarctic Ice Sheet Freshwater Discharge Drives Substantial Southern Ocean Changes Over the 21st Century, Geophysical Research Letters, 50, e2023GL104949, https://doi.org/10.1029/2023GL104949, 2023.
  - Greene, C. A., Gardner, A. S., Wood, M., and Cuzzone, J. K.: Ubiquitous acceleration in Greenland Ice Sheet calving from 1985 to 2022, Nature, 625, 523–528, https://doi.org/10.1038/s41586-023-06863-2, 2024.
- Han, Z., Power, K., Li, G., and Zhang, Q.: Impacts of Mid-Pliocene Ice Sheets and Vegetation on Afro-Asian Summer Monsoon Rainfall Revealed by EC-Earth Simulations, Geophysical Research Letters, 51, e2023GL106145, https://doi.org/10.1029/2023GL106145, 2024.
  - Haywood, Dowsett, H. J., Dolan, A. M., Rowley, D., Abe-Ouchi, A., Otto-Bliesner, B., Chandler, M. A., Hunter, S. J., Lunt, D. J., Pound, M., and Salzmann, U.: The Pliocene Model Intercomparison Project (PlioMIP) Phase 2: scientific objectives and experimental design, Climate of the Past, 12, 663–675, https://doi.org/10.5194/cp-12-663-2016, 2016.
- Haywood, Tindall, J. C., Dowsett, H. J., Dolan, A. M., Foley, K. M., Hunter, S. J., Hill, D. J., Chan, W.-L., Abe-Ouchi, A., Stepanek, C., Lohmann, G., Chandan, D., Peltier, W. R., Tan, N., Contoux, C., Ramstein, G., Li, X., Zhang, Z., Guo, C., Nisancioglu, K. H., Zhang, Q., Li, Q., Kamae, Y., Chandler, M. A., Sohl, L. E., Otto-Bliesner, B. L., Feng, R., Brady, E. C., von der Heydt, A. S., Baatsen, M. L. J., and Lunt, D. J.: The Pliocene Model Intercomparison Project Phase 2: large-scale climate features and climate sensitivity, Climate of the Past, 16, 2095–2123, https://doi.org/10.5194/cp-16-2095-2020, 2020.
- Haywood, A. M., Hill, D. J., Dolan, A. M., Otto-Bliesner, B. L., Bragg, F., Chan, W.-L., Chandler, M. A., Contoux, C., Dowsett, H. J., Jost, A., Kamae, Y., Lohmann, G., Lunt, D., Abe-Ouchi, A., Pickering, S. J., Ramstein, G., Rosenbloom, N., Salzmann, U., Sohl, L., Stepanek,

- C., Ueda, H., Yan, Q., and Zhang, Z.: Large-scale features of Pliocene climate: results from the Pliocene Model Intercomparison Project, Climate of the Past, 9, 191–209, https://doi.org/10.5194/cp-9-191-2013, 2013.
- Haywood, A. M., Tindall, J. C., Burton, L. E., Chandler, M. A., Dolan, A. M., Dowsett, H. J., Feng, R., Fletcher, T. L., Foley,
  K. M., Hill, D. J., Hunter, S. J., Otto-Bliesner, B. L., Lunt, D. J., Robinson, M. M., and Salzmann, U.: Pliocene Model Intercomparison Project Phase 3 (PlioMIP3) Science plan and experimental design, Global and Planetary Change, 232, 104316, https://doi.org/10.1016/j.gloplacha.2023.104316, 2024.
  - Hill, D.: Modelling Earth's cryosphere during Peak Pliocene Warmth, Ph.D. thesis, University of Bristol /British Antarctic Survey, 2009.
- Hill, D., Haywood, A., Hindmarsh, R., and Valdes, P.: Characterizing ice sheets during the Pliocene: evidence from data and models, in:
   Deep-Time Perspectives on Climate Change: Marrying the Signal from Computer Models and Biological Proxies, edited by Williams,
   M., Haywood, A., Gregory, F., and Schmidt, D., pp. 517–538, The Geological Society of London on behalf of The Micropalaeontological Society, first edn., https://doi.org/10.1144/TMS002.24, 2007.
  - Hosking, J. S., Orr, A., Marshall, G. J., Turner, J., and Phillips, T.: The Influence of the Amundsen–Bellingshausen Seas Low on the Climate of West Antarctica and Its Representation in Coupled Climate Model Simulations, Journal of Climate, 26, 6633–6648, https://doi.org/10.1175/JCLI-D-12-00813.1, 2013.

535

- Hutchinson, D. K., Menviel, L., Meissner, K. J., and Hogg, A. M.: East Antarctic warming forced by ice loss during the Last Interglacial, Nature Communications, 15, 1026, https://doi.org/10.1038/s41467-024-45501-x, 2024.
- Johnson, G. C., Mahmud, A. K. M. S., Macdonald, A. M., and Twining, B. S.: Antarctic Bottom Water Warming, Freshening, and Contraction in the Eastern Bellingshausen Basin, Geophysical Research Letters, 51, e2024GL109 937, https://doi.org/10.1029/2024GL109937, 2024.
- Kang, S. M., Yu, Y., Deser, C., Zhang, X., Kang, I.-S., Lee, S.-S., Rodgers, K. B., and Ceppi, P.: Global impacts of recent Southern Ocean cooling, Proceedings of the National Academy of Sciences, 120, e2300881120, https://doi.org/10.1073/pnas.2300881120, 2023.
  - Kidston, J., Vallis, G. K., Dean, S. M., and Renwick, J. A.: Can the Increase in the Eddy Length Scale under Global Warming Cause the Poleward Shift of the Jet Streams?, Journal of Climate, 24, 3764–3780, https://doi.org/10.1175/2010JCLI3738.1, 2011.
  - Kim, S. and Crowley, T. J.: Increased Pliocene North Atlantic Deep Water: Cause or consequence of Pliocene warming?, Paleoceanography, 15, 451–455, https://doi.org/10.1029/1999PA000459, 2000.
  - Koenigk, T., Brodeau, L., Graversen, R. G., Karlsson, J., Svensson, G., Tjernström, M., Willén, U., and Wyser, K.: Arctic climate change in 21st century CMIP5 simulations with EC-Earth, Climate Dynamics, 40, 2719–2743, https://doi.org/10.1007/s00382-012-1505-y, 2013.
  - Kusahara, K., Williams, G. D., Tamura, T., Massom, R., and Hasumi, H.: Dense shelf water spreading from <span style="font-variant:small-caps;">A</span> ntarctic coastal polynyas to the deep <span style="font-variant:small-caps;">S</span> outhern <span style="font-variant:small-caps;">O</span> cean: A regional circumpolar model study, Journal of Geophysical Research: Oceans, 122, 6238–6253, https://doi.org/10.1002/2017JC012911, 2017.
  - Lord, N. S., Crucifix, M., Lunt, D. J., Thorne, M. C., Bounceur, N., Dowsett, H., O'Brien, C. L., and Ridgwell, A.: Emulation of long-term changes in global climate: application to the late Pliocene and future, Climate of the Past, 13, 1539–1571, https://doi.org/10.5194/cp-13-1539-2017, 2017.
- Lunt, D. J., Haywood, A. M., Schmidt, G. A., Salzmann, U., Valdes, P. J., Dowsett, H. J., and Loptson, C. A.: On the causes of mid-Pliocene warmth and polar amplification, Earth and Planetary Science Letters, 321-322, 128–138, https://doi.org/10.1016/j.epsl.2011.12.042, 2012.
  - Marshall, G. J.: Trends in the Southern Annular Mode from Observations and Reanalyses, Journal of Climate, 16, 4134–4143, https://doi.org/10.1175/1520-0442(2003)016<4134:TITSAM>2.0.CO;2, 2003.

- Menviel, L. C., Spence, P., Kiss, A. E., Chamberlain, M. A., Hayashida, H., England, M. H., and Waugh, D.: Enhanced Southern

  Ocean CO<sub>2</sub> outgassing as a result of stronger and poleward shifted southern hemispheric westerlies, Biogeosciences, 20, 4413–4431, 
  https://doi.org/10.5194/bg-20-4413-2023, 2023.
  - Naish, T., Powell, R., Levy, R., Wilson, G., Scherer, R., Talarico, F., Krissek, L., Niessen, F., Pompilio, M., Wilson, T., Carter, L., DeConto, R., Huybers, P., McKay, R., Pollard, D., Ross, J., Winter, D., Barrett, P., Browne, G., Cody, R., Cowan, E., Crampton, J., Dunbar, G., Dunbar, N., Florindo, F., Gebhardt, C., Graham, I., Hannah, M., Hansaraj, D., Harwood, D., Helling, D., Henrys, S., Hinnov, L., Kuhn, G.,
- Kyle, P., Läufer, A., Maffioli, P., Magens, D., Mandernack, K., McIntosh, W., Millan, C., Morin, R., Ohneiser, C., Paulsen, T., Persico, D., Raine, I., Reed, J., Riesselman, C., Sagnotti, L., Schmitt, D., Sjunneskog, C., Strong, P., Taviani, M., Vogel, S., Wilch, T., and Williams, T.: Obliquity-paced Pliocene West Antarctic ice sheet oscillations, Nature, 458, 322–328, https://doi.org/10.1038/nature07867, 2009.
  - Naughten, K. A., Holland, P. R., and De Rydt, J.: Unavoidable future increase in West Antarctic ice-shelf melting over the twenty-first century, Nature Climate Change, 13, 1222–1228, https://doi.org/10.1038/s41558-023-01818-x, 2023.
- Orsi, A., Johnson, G., and Bullister, J.: Circulation, mixing, and production of Antarctic Bottom Water, Progress in Oceanography, 43, 55–109, https://doi.org/10.1016/S0079-6611(99)00004-X, 1999.
  - Pollard, D., DeConto, R. M., and Alley, R. B.: Potential Antarctic Ice Sheet retreat driven by hydrofracturing and ice cliff failure, Earth and Planetary Science Letters, 412, 112–121, https://doi.org/10.1016/j.epsl.2014.12.035, 2015.
- Power, K. and Zhang, Q.: The impacts of reduced ice sheets, vegetation, and elevated CO2 on future Arctic climates, Arctic, Antarctic, and Alpine Research, 56, 2433 860, https://doi.org/10.1080/15230430.2024.2433860, 2024.
  - Power, K., Lu, Z., and Zhang, Q.: Impacts of large-scale Saharan solar farms on the global terrestrial carbon cycle, Environmental Research Letters, 18, 104 009, https://doi.org/10.1088/1748-9326/acf7d8, 2023.
  - Ramadhan, A., Marshall, J., Meneghello, G., Illari, L., and Speer, K.: Observations of Upwelling and Downwelling Around Antarctica Mediated by Sea Ice, Frontiers in Marine Science, 9, 864 808, https://doi.org/10.3389/fmars.2022.864808, 2022.
- Raphael, M. N., Marshall, G. J., Turner, J., Fogt, R. L., Schneider, D., Dixon, D. A., Hosking, J. S., Jones, J. M., and Hobbs, W. R.: The Amundsen Sea Low: Variability, Change, and Impact on Antarctic Climate, Bulletin of the American Meteorological Society, 97, 111–121, https://doi.org/10.1175/BAMS-D-14-00018.1, 2016.

- Roach, L. A., Mankoff, K. D., Romanou, A., Blanchard-Wrigglesworth, E., Haine, T. W. N., and Schmidt, G. A.: Winds and Meltwater Together Lead to Southern Ocean Surface Cooling and Sea Ice Expansion, Geophysical Research Letters, 50, e2023GL105948, https://doi.org/10.1029/2023GL105948, 2023.
- Schmidt, C., Morrison, A. K., and England, M. H.: Wind– and Sea-Ice–Driven Interannual Variability of Antarctic Bottom Water Formation, Journal of Geophysical Research: Oceans, 128, e2023JC019774, https://doi.org/10.1029/2023JC019774, 2023.
- Screen, J. A., Simmonds, I., and Keay, K.: Dramatic interannual changes of perennial Arctic sea ice linked to abnormal summer storm activity, Journal of Geophysical Research, 116, D15 105, https://doi.org/10.1029/2011JD015847, 2011.
- Sidorenko, D., Danilov, S., Streffing, J., Fofonova, V., Goessling, H. F., Scholz, P., Wang, Q., Androsov, A., Cabos, W., Juricke, S., Koldunov, N., Rackow, T., Sein, D. V., and Jung, T.: AMOC Variability and Watermass Transformations in the AWI Climate Model, Journal of Advances in Modeling Earth Systems, 13, e2021MS002582, https://doi.org/10.1029/2021MS002582, 2021.
  - Silvano, A., Purkey, S., Gordon, A. L., Castagno, P., Stewart, A. L., Rintoul, S. R., Foppert, A., Gunn, K. L., Herraiz-Borreguero, L., Aoki, S., Nakayama, Y., Naveira Garabato, A. C., Spingys, C., Akhoudas, C. H., Sallée, J.-B., De Lavergne, C., Abrahamsen, E. P., Meijers, A.
- J. S., Meredith, M. P., Zhou, S., Tamura, T., Yamazaki, K., Ohshima, K. I., Falco, P., Budillon, G., Hattermann, T., Janout, M. A., Llanillo, P., Bowen, M. M., Darelius, E., Østerhus, S., Nicholls, K. W., Stevens, C., Fernandez, D., Cimoli, L., Jacobs, S. S., Morrison, A. K., Hogg,

- A. M., Haumann, F. A., Mashayek, A., Wang, Z., Kerr, R., Williams, G. D., and Lee, W. S.: Observing Antarctic Bottom Water in the Southern Ocean, Frontiers in Marine Science, 10, 1221 701, https://doi.org/10.3389/fmars.2023.1221701, 2023.
- Song, P., Scholz, P., Knorr, G., Sidorenko, D., Timmermann, R., and Lohmann, G.: Regional conditions determine thresholds of accelerated Antarctic basal melt in climate projection, Nature Climate Change, https://doi.org/10.1038/s41558-025-02306-0, 2025.
- Steig, E. J., Huybers, K., Singh, H. A., Steiger, N. J., Ding, Q., Frierson, D. M. W., Popp, T., and White, J. W. C.: Influence of West Antarctic Ice Sheet collapse on Antarctic surface climate, Geophysical Research Letters, 42, 4862–4868, https://doi.org/10.1002/2015GL063861, 2015.
- Talley, L.: Distribution and Formation of North Pacific Intermediate Water, Journal of Physical Oceanography, 23, 517–537, 1993.

- Tamsitt, V., Drake, H. F., Morrison, A. K., Talley, L. D., Dufour, C. O., Gray, A. R., Griffies, S. M., Mazloff, M. R., Sarmiento, J. L., Wang, J., and Weijer, W.: Spiraling pathways of global deep waters to the surface of the Southern Ocean, Nature Communications, 8, 172, https://doi.org/10.1038/s41467-017-00197-0, 2017.
  - Thompson, D. W. J. and Wallace, J. M.: Annular Modes in the Extratropical Circulation. Part I: Month-to-Month Variability\*, Journal of Climate, 13, 1000–1016, https://doi.org/10.1175/1520-0442(2000)013<1000:AMITEC>2.0.CO;2, 2000.
- Thompson, D. W. J., Baldwin, M. P., and Solomon, S.: Stratosphere–Troposphere Coupling in the Southern Hemisphere, Journal of the Atmospheric Sciences, 62, 708–715, https://doi.org/10.1175/JAS-3321.1, 2005.
  - Weiffenbach, J. E., Dijkstra, H. A., Von Der Heydt, A. S., Abe-Ouchi, A., Chan, W.-L., Chandan, D., Feng, R., Haywood, A. M., Hunter, S. J., Li, X., Otto-Bliesner, B. L., Peltier, W. R., Stepanek, C., Tan, N., Tindall, J. C., and Zhang, Z.: Highly stratified mid-Pliocene Southern Ocean in PlioMIP2, Climate of the Past, 20, 1067–1086, https://doi.org/10.5194/cp-20-1067-2024, 2024.
- Yao, S.-L., Wu, R., Luo, J.-J., and Zhou, W.: Competing impacts of tropical Pacific and Atlantic on Southern Ocean inter-decadal variability, npj Climate and Atmospheric Science, 7, 104, https://doi.org/10.1038/s41612-024-00662-w, 2024.
  - Yeung, N. K.-H., Menviel, L., Meissner, K. J., Choudhury, D., Ziehn, T., and Chamberlain, M. A.: Last Interglacial subsurface warming on the Antarctic shelf triggered by reduced deep-ocean convection, Communications Earth & Environment, 5, 212, https://doi.org/10.1038/s43247-024-01383-x, 2024.
- Zhang, L., Delworth, T. L., Cooke, W., and Yang, X.: Natural variability of Southern Ocean convection as a driver of observed climate trends, Nature Climate Change, 9, 59–65, https://doi.org/10.1038/s41558-018-0350-3, 2019.
  - Zhang, Q., Berntell, E., Axelsson, J., Chen, J., Han, Z., de Nooijer, W., Lu, Z., Li, Q., Zhang, Q., Wyser, K., and Yang, S.: Simulating the mid-Holocene, last interglacial and mid-Pliocene climate with EC-Earth3-LR, Geoscientific Model Development, 14, 1147–1169, https://doi.org/10.5194/gmd-14-1147-2021, 2021.